

Improved silicon surface passivation achieved by negatively charged silicon nitride films

K. J. Weber^{a)} and H. Jin

Centre for Sustainable Energy Systems, Faculty of Engineering and Information Technology, The Australian National University, Canberra, Australian Capital Territory 0200, Australia

(Received 18 September 2008; accepted 8 January 2009; published online 11 February 2009)

A corona discharge is used to create and store negative charge in the silicon nitride films of silicon dioxide/silicon nitride stacks. Effective lifetime measurements on both textured and planar, as well as both boron diffused and undiffused silicon samples passivated with silicon oxide/silicon nitride stacks, show that the creation of negative charge in the nitride layer results in an improvement in the surface passivation for all samples, with very low (<2 cm/s) effective surface recombination velocities demonstrated for planar, undiffused samples. The manipulation of charge can be exploited to improve the conversion efficiency of silicon solar cells. © 2009 American Institute of Physics. [DOI: 10.1063/1.3077157]

The charge density of dielectric layers used as antireflection coatings and surface passivation layers in silicon solar cells—chiefly silicon nitride (SiN_x) deposited by plasma enhanced chemical vapor deposition (PECVD)—is well known to substantially influence the degree of surface passivation achieved. PECVD SiN_x usually contains a significant density of positive charge (typically several 10^{12} cm^{-2}). This positive charge is beneficial for the passivation of the n type emitter of conventional solar cells on p type substrates. However, positive charge is not ideal for the passivation of the rear of such cells due to the formation of an inversion layer, which introduces additional losses as well as a virtual shunt.¹ Additionally, solar cells featuring a p type emitter would benefit from passivation with a dielectric containing negative charge. There is thus great interest in the realization of negative charge in dielectrics. Recently Hoex *et al.*^{2,3} showed that plasma assisted atomic layer deposited (ALD) Al_2O_3 layers can provide good surface passivation for p type emitters as well as for undiffused surfaces because these Al_2O_3 layers contain a high density of negative charge. A disadvantage is that ALD is a slow process, making the industrial applicability of the process uncertain.

The dominant defect in stoichiometric and silicon rich SiN_x films is known to be the K center, consisting of a Si atom backbonded to three N atoms.⁴ It is now well established that this defect is responsible for the net positive charge in these films. Further, it is known that the K center is amphoteric⁵ and displays a negative correlation energy such that the charged states (K^+ and K^-) are more stable than the neutral state (K^0).⁶ The charge state of the K center can be easily manipulated by charge injection from the silicon substrate, and this fact has been exploited for nonvolatile memory devices.^{7,8} A key requirement for the storage of charge (other than the as-deposited charge) in silicon nitride is the presence of a barrier layer such as silicon dioxide, which prevents the leakage of charge back into the silicon substrate.

The manipulation of the charge in SiN_x films offers significant potential advantages for photovoltaic applications since SiN_x deposition is an industry standard process and

these films have a unique set of properties, including an optimal refractive index and (in the case of PECVD deposited nitride) a high hydrogen content, which can be used to passivate bulk defects. The ability to engineer the charge in the film at the end of the process—following film deposition and subsequent thermal treatments—would thus significantly enhance process flexibility. However, this ability has not been exploited to date. In this paper, we investigate the effect of negative charge storage in silicon nitride films on interface recombination for both undiffused and boron diffused, as well as textured and planar silicon substrates.

Float zoned, p type, (100) >100 Ω cm, ~ 500 μm thick c -Si wafers are used as the starting material for samples used for lifetime measurements. Selected samples were randomly textured with upright pyramids using an alkaline solution. After a standard Radio Corporation of American clean, a boron diffusion was performed on both sides of selected samples using a liquid boron tribromide source at a temperature of 900–950 °C to obtain a sheet resistance of around 200 Ω/\square . The surface doping density is around $4 \times 10^{18}/\text{cm}^3$ after all thermal steps. An oxide layer around 20 nm thick was then thermally grown on both sides at 1000 °C on all samples, followed by a forming gas anneal (FGA, 4% H_2 in Ar) at 400 °C for 30 min. ~ 50 nm stoichiometric silicon nitride (Si_3N_4) was deposited on both sides of all samples using low pressure CVD (LPCVD) at 775 °C and 0.5 Torr, with an ammonia to dichlorosilane flow ratio of 4:1.

Samples used for C - V measurements were Cz p -type, 10–15 Ω cm (100) wafers. After cleaning, the samples received the same oxidation, FGA and LPCVD nitride deposition as the lifetime samples.

Corona charging was carried out on lifetime and C - V samples with a conventional setup⁹ by applying voltage of +10 kV to a steel needle about 5 cm above the samples. Both sides of the samples were positively charged for 5 min. This results in the buildup of a high positive charge density on the surface of the oxide (estimated to be up to 10^{13} cm^{-2}). All samples were then rinsed in isopropanol (IPA) solution to remove the surface charges. The efficacy of an IPA dip in removing surface charge was verified independently. The positive corona charges result in a strong electric field, which causes the injection of electrons from the silicon into the

^{a)}Electronic mail: klaus.weber@anu.edu.au.

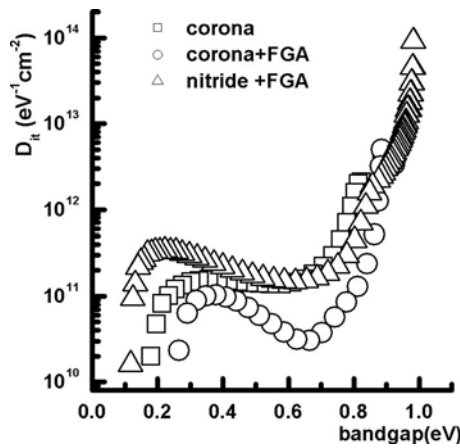


FIG. 1. Defect density distribution within the band gap for samples following various process steps. Step 1: LPCVD nitride deposition; step 2: subsequent corona charging and IPA rinse; and step 3: subsequent 400 °C anneal.

nitride where they are trapped at the *K* centers. The IPA solution then removes the positive charges at the nitride surface, leaving only the negative charges in the structure.

Selected samples received an anneal at 400 °C for 5 min. The low temperature anneal has the effect of eliminating certain defects that may be generated by corona charging.¹⁰ However, the anneal does not result in the diffusion of any atmospheric species, such as H₂, to the Si–SiO₂ interface since the nitride layer forms an efficient diffusion barrier.^{11,12} The anneal temperature is also too low to result in the liberation of significant quantities of hydrogen from the nitride film.¹¹

The oxide and nitride layers were removed from the rear of the *C-V* samples. Before *C-V* measurements, 80 nm Al was thermally evaporated through a shadow mask on the nitride surface to form a Metal-Insulator-Semiconductor structure, and a Ga/In paste was applied to the rear to make electrical contact to the Si bulk. High frequency (1 MHz) and quasistatic *C-V* measurements were performed.

Lifetime measurements were carried out using the inductively coupled photoconductivity decay technique,^{13,14} and both the effective lifetime τ_{eff} and the emitter saturation current density J_{oe} were determined, as described elsewhere.¹⁵

Figure 1 shows the defect density distributions extracted from the *C-V* curves of the samples following various process steps: (i) just after LPCVD nitride deposition and anneal; (ii) corona charging and IPA dip following LPCVD nitride deposition; and (iii) corona charging, IPA dip, and a subsequent anneal following LPCVD nitride deposition. Table I summarizes the flat band voltage (V_{fb}), effective charge density (Q_{eff}), and defect density at mid gap [$D_{it}(m)$] following the same process steps. Q_{eff} was determined assuming that all the charge resides at the SiO₂–Si₃N₄ interface. In practice, the charge is likely to be distributed

TABLE I. Flat band voltage V_{fb} , effective charge density Q_{eff} and mid gap defect density $D_{it}(m)$ for samples following various process treatments.

Process step	V_{fb} (V)	Q_{eff} (10 ¹¹ cm ⁻²)	$D_{it}(m)$ (10 ¹⁰ eV ⁻¹ cm ⁻²)
Nitride deposition	-1.7	+7	14
Corona charging	+4.3	-43	14
400 °C anneal	+2.2	-26	4.5

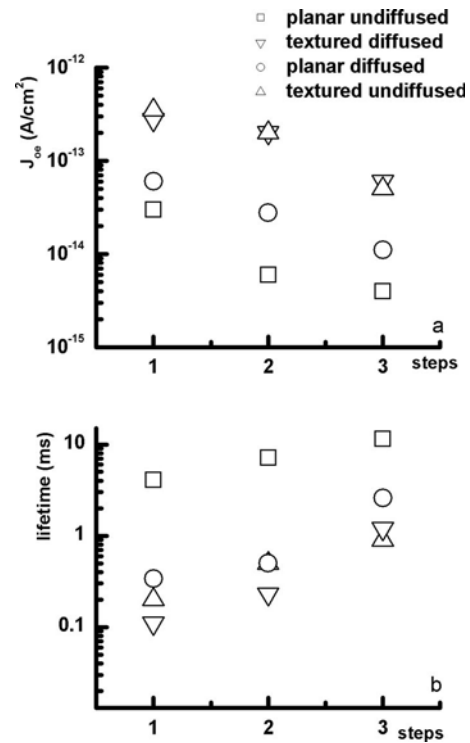


FIG. 2. Emitter saturation current density (a) and effective lifetime (b) following various process steps. Step 1: LPCVD nitride deposition; step 2: subsequent corona charging and IPA rinse; and step 3: subsequent 400 °C anneal. All lifetimes were measured at an injection level of $5 \times 10^{14}/\text{cm}^3$, while J_{oe} was measured at an injection level of $4 \times 10^{15}/\text{cm}^3$.

throughout the nitride, which would require higher charge densities to account for the observed flat band voltages.

Before corona charging, the net effective charge in the silicon nitride film is positive. The positive corona charging and IPA steps result in a net negative charge due to the injection of electrons across the oxide and into the nitride film, where they are trapped at the *K* centers, according to the reactions $K^+ + 2e^- \rightarrow K^-$ and $K^0 + e^- \rightarrow K^-$.¹⁶ The subsequent anneal reduces the charge density due to the detrapping of electrons from *K*⁻ centers at elevated temperatures and transport across the barrier oxide.

The corona charging process appears to result in some changes in the interface defect density distribution but no significant increase in their density. The subsequent anneal reduces the defect density below the level prior to corona charging. The mechanism responsible for this decrease is not understood at present. It is known that the LPCVD silicon nitride deposition process results in some dehydrogenation of the interface.¹² It is possible that energetic electrons that are injected into the nitride film result in the release of hydrogen.¹⁷ Following the anneal, the liberated hydrogen may be able to passivate defects at the Si–SiO₂ interface. It should be noted that as-deposited LPCVD nitride has been shown to be stable and not affected by an FGA up to 450 °C.¹⁸ Our own experimental data confirm that anneals at 400 °C do not affect the *C-V* curves and lifetime/ J_{oe} results for samples without corona charging.

Figure 2(a) shows the change in J_{oe} following various process steps, while Fig. 2(b) shows the corresponding lifetime values. J_{oe} values can only be extracted from lifetime measurements under conditions where the wafer bulk is in high level injection and the surface remains in low level

injection. For diffused samples, this condition is always met. For undiffused samples, we determined the surface concentrations of majority carriers (electrons for the as-deposited sample with a net positive charge, holes for samples following corona charging and IPA dip) using the charge densities calculated in Table I. These values are 1.7×10^{18} , 2.8×10^{19} , and $7.8 \times 10^{19} \text{ cm}^{-3}$ following steps 1, 2, and 3 in Fig. 2, respectively. These carrier densities are sufficiently high to satisfy the conditions for J_{oe} measurement.

Figure 2 clearly demonstrates that the negatively charged nitride/oxide layers display improved surface passivation for all the samples investigated. The upper limit of the effective surface recombination velocity S_{eff} can be calculated by assuming an infinite bulk lifetime

$$S_{\text{eff}} < W/2\tau_{\text{eff}}, \quad (1)$$

where W is the sample thickness and τ_{eff} is the effective lifetime. We determine values of S_{eff} of less than 2 and 22 cm/s for planar and textured undiffused Si surfaces, respectively, at an injection level of $5 \times 10^{14} \text{ cm}^{-3}$. For boron diffused emitters, J_{oe} values of 10 and 60 fA/cm² per side are achieved for planar and textured Si surfaces, respectively. It is also interesting to note that the J_{oe} and effective lifetime improve following the 400 °C anneal despite a reduction in the negative charge density in the film. In this case, it appears that the benefit resulting from a reduction in interface defect density outweighs the disadvantage associated with a reduction in the charge density in the film.

There are other interesting features that can be discerned from the data in Fig. 2, such as the clustering of some of the lifetime and J_{oe} values. This is most pronounced for the J_{oe} values of the textured samples. This may be due to the fact that according to modeling, the surface minority carrier concentrations are quite similar for diffused and undiffused samples under all conditions. However, no such clustering is observed for the planar samples. Further work will be required to obtain a more detailed understanding of the data presented in Fig. 2.

Preliminary results indicate that the negative charges in this nitride/oxide structure are sufficiently stable for photovoltaic applications. We have observed no change in the effective lifetimes of our samples after storage for 48 h at 150 °C.

In conclusion, we have shown that the introduction of negative charge into silicon nitride layers can be used to improve the surface passivation of p type silicon surfaces and is a promising method for the improvement of solar cell efficiency.

Support for this work from the Australian Research Council (ARC Discovery Grant No. DP0664357) is gratefully acknowledged.

- ¹S. Dauwe, L. Mittelstadt, A. Metz, and R. Hezel, *Prog. Photovoltaics* **10**, 271 (2002).
- ²B. Hoex, J. Schmidt, R. Bock, P. P. Altermatt, M. C. M. van de Sanden, and W. M. M. Kessels, *Appl. Phys. Lett.* **91**, 112107 (2007).
- ³B. Hoex, S. B. S. Heil, E. Langereis, M. C. M. van de Sanden, and W. M. M. Kessels, *Appl. Phys. Lett.* **89**, 042112 (2006).
- ⁴W. L. Warren and P. M. Lenahan, *Phys. Rev. B* **42**, 1773 (1990).
- ⁵D. T. Krick, P. M. Lenahan, and J. Kanicki, *Phys. Rev. B* **38**, 8226 (1988).
- ⁶P. M. Lenahan, D. T. Krick, and J. Kanicki, *Appl. Surf. Sci.* **39**, 392 (1989).
- ⁷M. H. White, Y. L. Yang, A. Purwar, and M. L. French, *IEEE Trans. Compon., Packag. Manuf. Technol., Part A* **20**, 190 (1997).
- ⁸Y. L. Yang and M. H. White, *Solid-State Electron.* **44**, 949 (2000).
- ⁹Z. A. Weinberg, W. C. Johnson, and M. A. Lampert, *J. Appl. Phys.* **47**, 248 (1976).
- ¹⁰H. Jin, K. J. Weber, N. C. Dang, and W. E. Jellett, *Appl. Phys. Lett.* **90**, 262109 (2007).
- ¹¹W. M. Arnoldbik, C. H. M. Marée, A. J. H. Maas, M. J. van den Boogaard, F. H. P. M. Habraken, and A. E. T. Kuiper, *Phys. Rev. B* **48**, 5444 (1993).
- ¹²H. Jin, K. J. Weber, P. N. K. Deenanaray, and A. W. Blakers, *J. Electrochem. Soc.* **153**, G750 (2006).
- ¹³E. Yablonovitch and T. J. Gmitter, *Solid-State Electron.* **35**, 261 (1992).
- ¹⁴D. E. Kane and R. M. Swanson, Proceedings of the 18th IEEE Photovoltaic Specialists Conference, 1981 (unpublished).
- ¹⁵W. E. Jellett and K. J. Weber, *Appl. Phys. Lett.* **90**, 042104 (2007).
- ¹⁶S. E. Curry, P. M. Lenahan, D. T. Krick, J. Kanicki, and C. T. Kirk, *Appl. Phys. Lett.* **56**, 1359 (1990).
- ¹⁷E. Cartier and J. H. Stathis, *Appl. Phys. Lett.* **69**, 103 (1996).
- ¹⁸J. Z. Xie, S. P. Murarka, X. S. Guo, and W. A. Lanford, *J. Vac. Sci. Technol. B* **7**, 150 (1989).